Journal of Power Sources 184 (2008) 432–436

Contents lists available at ScienceDirect

Journal of Power Sources

journal homepage: www.elsevier.com/locate/jpowsour

Short communication

Coating of multi-walled carbon nanotube with SnO_2 films of controlled thickness and its application for Li-ion battery

Zhenyao Wang, Ge Chen, Dingguo Xia *

College of Environmental and Energy Engineering, Beijing University of Technology, Beijing 100022, China

ARTICLE INFO

Article history:
Received 4 January 2008
Received in revised form 16 March 2008
Accepted 18 March 2008
Available online 22 March 2008

Keywords:
Tin oxide
Multi-walled carbon nanotubes
Lithium-ion battery
Thickness controlling

ABSTRACT

Multi-walled carbon nanotubes (MWCNTs) coated with a smooth and uniform tin oxide (SnO_2) layers of different thickness were prepared by a novel thioglycolic acid assisted one-step wet chemical method. The coatings were characterized by powder X-ray diffraction (XRD) and transmission electron microscopy (TEM). The thickness of the SnO_2 coatings can be easily controlled by changing the synthesis conditions, such as pH value of the solution and hydrolysis time. The electrochemical properties of the SnO_2/MWCNTs composites as anode materials for lithium batteries were studied by galvanostatic method. The composites showed high charge capacities and good durability against decay. This could be ascribed to the good dispersion, thin layer and small particle size of SnO_2 on MWCNTs.

1. Introduction

SnO_2 is an n-type semiconductor oxide with a wide band gap (E_g = 3.6 eV at 300 K) and plays a key role in applications, such as gas sensors, solar cells, catalysts, conductive electrodes, transparent coatings, and hydrogenation [1–4]. Tin oxide-based materials, as possible candidates for the next generation of anode materials for Li-ion batteries due to their high-lithium storage capacity and low potential of lithium ion intercalation, have drawn considerable interest [5]. A SnO_2 anode can give a maximum theoretical 781 mAh g^{-1} charge-storage capacity, which is over twice as much Li^+ as the carbon anodes (372 mAh g^{-1}) [6]. However, a major problem of anode materials for lithium ion batteries is the significant volume change occurring during the alloying and dealloying processes, which may induce damage to the anodes and cause very poor long-term cyclability. Moreover, the formation of amorphous Li_2O matrix causes a huge irreversible capacity during the first cycle [7–10]. In order to improve the stability and cycle life, different proposals have been undertaken. It was reported that small and uniform distribution of particles tends to minimize the dimensional changes and pulverization failure of SnO_2 anodes and, thereby, give improved performance [11–13]. However, the agglomeration of small particles during use can easily nullify the stated advantages [14]. SnO_2 nanofibers [15] and thin-film [16,17] have also been reported to effectively accommodate the volume change and show good cycling stability. Recently, several authors have explored the use of composites of SnO_2 and carbonaceous materials to ease the rapid capacity fading [12,13,18,19].

Carbon nanotubes have some excellent mechanical and electrical properties. As a new anode material for lithium-ion batteries, it shows good cycle stability, but large, irreversible capacity loss in the first cycle [20]. Moreover, it is reasonable to expect that multi-walled carbon nanotubes (MWCNTs)-supported SnO_2 could show good performances in using as anode material for lithium-ion batteries, though it is so strange that there are few reports about it [6].

Here, we report the surface coating of MWCNTs with a different thickness of SnO_2 layer by a novel thioglycolic acid assisted one-step wet chemical method. We first report the use of thioglycolic acid as the connecter to improve the uniformity of the layers. The thickness of the coating can be easily controlled by change the solution pH value, reactive time and the concentration of reactants. SnO_2/MWCNTs composites were used as anode materials for lithium-ion batteries and showed high charge capacities and good durability.

2. Experimental

2.1. Sample preparation

In a typical synthesis, 60 mg MWCNTs were first dispersed in 50 ml nitric acid (40%) and refluxed at 120 °C for 12 h under stirring to clean the nanotubes' surfaces. This acid-treated MWCNTs were

* Corresponding author. Tel.: +86 10 67396158; fax: +86 10 67396158.
E-mail address: dgxia@bjut.edu.cn (D. Xia).

0378-7753/$ – see front matter © 2008 Elsevier B.V. All rights reserved.
doi:10.1016/j.jpowsour.2008.03.028

Table 1
The prepared conditions of SnO_2/MWCNTs composites

Samples	Thioglycolic acid (mM)	HCl (38%) (ml)	Temperature	Time (h)
SC1	10	0.7	RT[a]	6
SC2	5	0.1	RT	6
SC3	10	0.1	RT	18
SC4	10	0.3 (+0.5 g urea)	60 °C	6

[a] Room temperature.

rinsed with distilled H_2O until the pH value of the solution close to neutral and then dried at 60 °C. 40 mg acid-treated MWCNTs were added into 40 ml thioglycolic acid solution and sonicated for about 30 min. Subsequently, certain amount of concentrated HCl (38%) and 1 g $SnCl_2 \cdot H_2O$ was added (in some cases, 0.5 g urea was added). The mixture solution was continued stirring for certain time (as listed in Table 1, 18 h for sample SC3 and 6 h for the others). Then, the treated MWCNTs were rinsed with distilled H_2O and dried at 60 °C. As listed in Table 1, SC1, SC2, SC3, and SC4 were used to denote the samples prepared in different conditions. Furthermore, all the samples were heated at 400 °C for 2 h in air, which were denoted by SC1a, SC2a, SC3a and SC4a, respectively.

2.2. Sample characterization

Transmission electron microscopy (TEM) images were taken with a JEOL 2010 microscope on powder samples deposited onto a copper micro-grid coated with holey carbon. An accelerating voltage of 200 kV was used. X-ray diffraction (XRD) patterns of sample powder were recorded on a Bruker D8 ADVANCE X-ray diffractometer. Cu Kα radiation and a fixed power source (35 kV, 35 mA) were used.

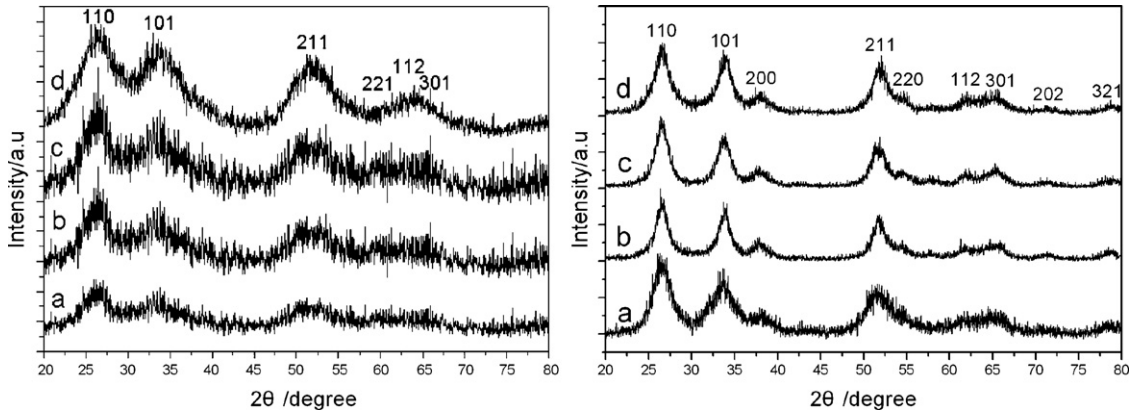

Fig. 1. The XRD patterns of SnO_2-coated MWCNTs before heat-treated (left): (a) SC1, (b) SC2, (c) SC3, and (d) SC4 and after heat-treated (right): (a) SC1a, (b) SC2a, (c) SC3a, and (d) SC4a.

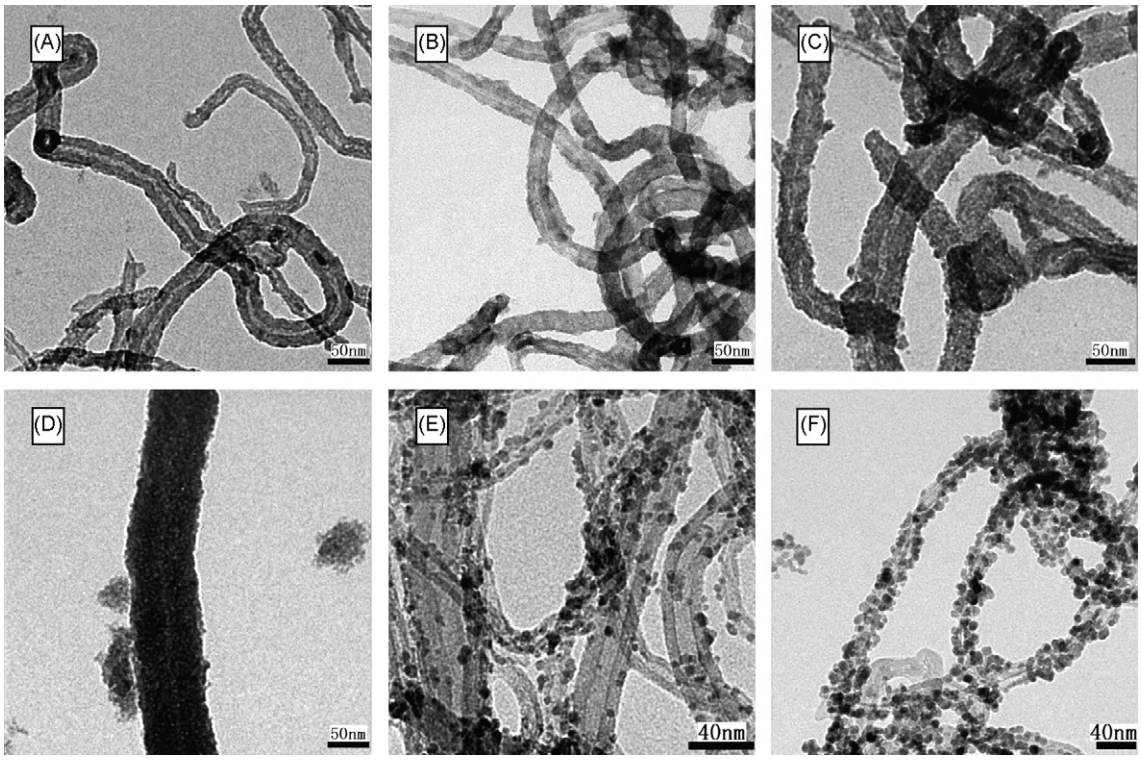

Fig. 2. TEM images of the different SnO_2/MWCNTs composites: (A) SC1, (B) SC2, (C) SC3, (D) SC4, (E) SC1a and (F) SC3a.

2.3. Electrochemical measurements

A *N*-methyl pyrrolidinone (NMP) slurry consisting of 80 wt% of the composite powder (various samples), 15 wt% of carbon black and 5 wt% polyvinylidene fluoride (Aldrich) was uniformly applied to a stainless steel disk of 16 mm in diameters. The disk electrodes were vacuum dried overnight at 120 °C. They were then assembled into Li test cells using 0.75 mm lithium foil as the negative electrode, microporous polypropylene separator, and an electrolyte of 1 M $LiPF_6$ in a 50:50 (w/w) mixture of ethylene carbonate (EC) and diethyl carbonate (DEC). Cell assembly was carried out in a re-circulating argon glove box where both the moisture and oxygen contents were below 1 ppm each. All cells were tested at the constant rate of 0.1 C and were charged and discharged between fixed voltage limits (2–0.1 V) on a Neware Technology limited battery testing system.

3. Results and discussion

3.1. Characterization of the SnO_2-coated MWCNTs

Fig. 1 (left) shows the XRD patterns of the SnO_2-coated MWCNTs composites before heat-treatment; in which a–d correspond

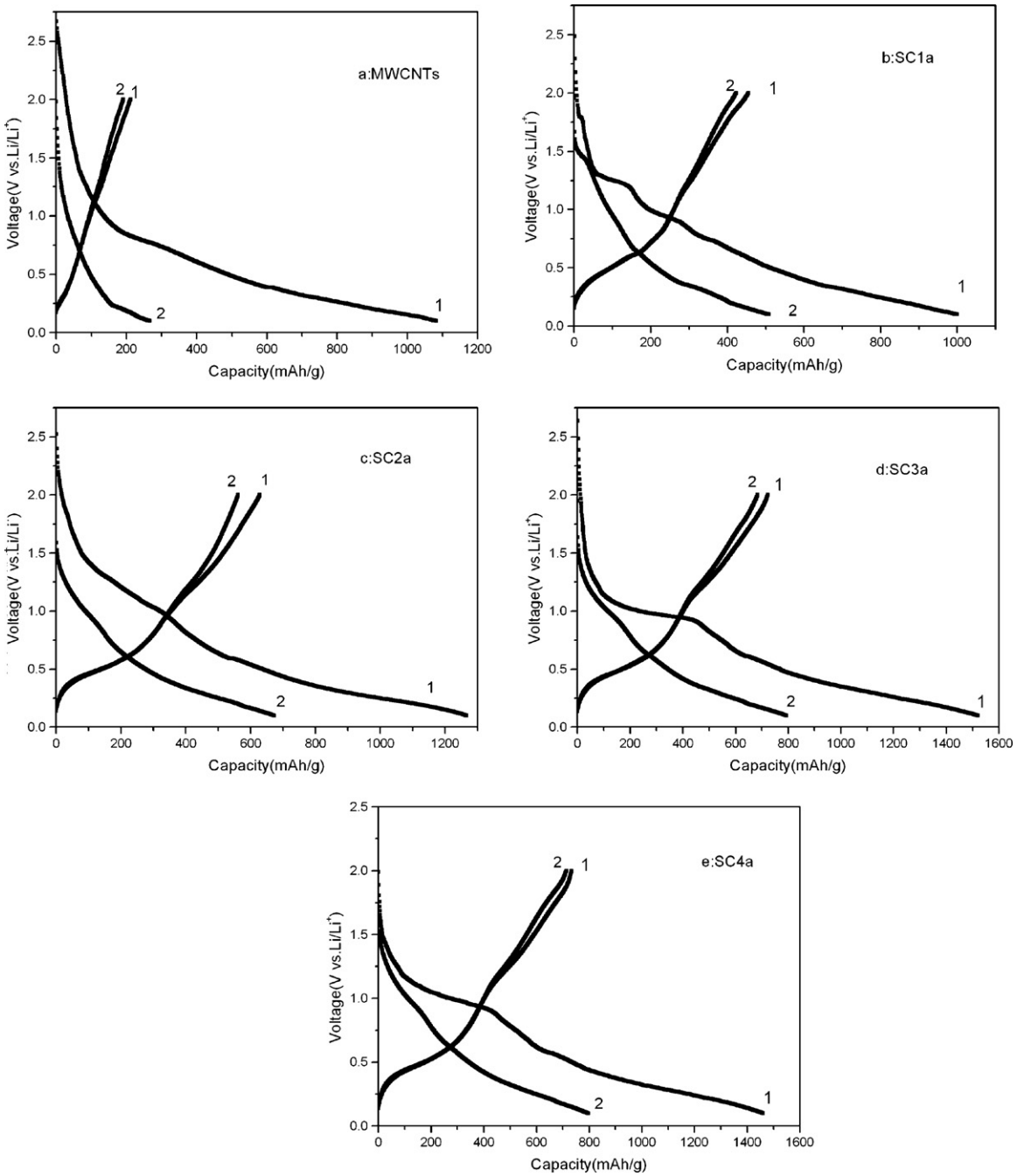

Fig. 3. The first two-cycle's discharge/charge curves of the samples (discharge/charge rate = 0.1 C, with voltage limit set at 2.0–0.1 V vs. Li/Li^+).

to sample SC1, SC2, SC3, and SC4, respectively. The diffraction angles at $2\theta = 26.3^\circ$, 33.6°, 51.8°, and 65.2° can be assigned to (1 1 0), (1 0 1), (2 1 1), and (3 0 1) planes of the cassiterite structure of SnO_2, respectively (JCPDS card no. 41-1445). The very broad peaks in the XRD pattern of SnO_2/MWCNTs composites before heat-treatment indicate that the coating SnO_2 particles show a small size or amorphous phase. The mean crystal size of SnO_2 calculated by Scherrer equation from (1 1 0) plane is about 2 nm. No obvious peaks corresponding to $SnCl_2$, Sn, or other impurities are observed in the powder patterns. As seen in Fig. 1 (right), the peak intensities of this composites become sharper and higher after heat-treatment at 400 °C for 2 h in air. The increase in intensity amplitude and decrease in width of the peaks reflect the increased crystalline and enlarged crystallite dimensions caused by the heat-treatment. The mean crystal sizes of heat-treated samples calculated by Scherrer equation from (1 1 0) plane are 3.7 ± 0.1 nm, 4.5 ± 0.1 nm, 4.8 ± 0.1 nm, and 4.9 ± 0.1 nm for SC1a, SC2a, SC3a, and SC4a, respectively.

Fig. 2 shows the TEM images of the different SnO_2-coated MWCNTs samples. A–F correspond to sample SC1, SC2, SC3, SC4, SC1a, and SC3a, respectively. It can be observed that almost all MWCNTs in the samples prepared by using thioglycolic acid have been fully coated with smooth and uniform tin oxide layers, without cracks and broken segments. For all of the samples, the size of SnO_2 grain coating on the MWCNTs is estimated to be 2 nm, which is consistent with the XRD results. Chemical analysis using EDS indicates the presence of Sn, O, C, and S in the coated MWCNTs. The atomic ratio of O to Sn is close to 2, and the weight of the residue S is about 1% of the total sample.

As seen from the TEM images, the thickness of SnO_2 layer before heat-treatment was estimated to be 1.8 nm, 3.3 nm, 5.3 nm, and 29 nm on average for SC1, SC2, SC3, SC4, respectively. The formation of SnO_2 particles should be attributed to the reaction of the precursor $SnCl_2 \cdot H_2O$ with residual oxygen in the reaction chamber as the following equation:

$$2\,SnCl_2 \cdot H_2O + O_2 \rightarrow 2\,SnO_2 + 4\,HCl$$

Firstly, the tin ions are adsorbed on the surface of the MWCNTs functionalized by the thioglycolic acid due to electrostatic attraction, and then in situ oxidized to become SnO_2 nanocrystals. The increasing thickness of the SnO_2 coating is ascribed to the continuous adsorption of tin ions on the as-originated SnO_2 coating and its slow crystallization [21]. It is obvious that the thickness of the SnO_2 coating increased with decreasing concentration of HCl in the hydrolysis solution, which was ascribed to the more complete hydrolysis of Sn^{2+} in dilute acidic solution. As for sample SC4, when urea was added, hydroxides produced from its hydrolysis at 60 °C make Sn^{2+} hydrolyze more completely. So the thickness of SnO_2 coating layer for sample SC4 is much thicker than that of other samples. The hydrolysis time is also effective on the thickness of the SnO_2 coating. When the time is extended to 18 h for SC3, it can be seen that the thickness extends to 5.3 nm, almost double that of SC2. After the samples were heat-treated, the SnO_2 coating aggregated to be bigger SnO_2 particles and studded on the MWCNTs surface separately.

3.2. Lithium electrochemical insertion study

The specific capacity and cycling stability of SnO_2/MWCNTs electrodes were measured by constant current charge/discharge testing. Fig. 3 shows the first two-cycle's discharge/charge curves of the MWCNT and SnO_2/MWCNTs composites, in which, a–e correspond to MWCNTs and sample SC1a–SC4a, respectively. Cycling was performed at a discharge/charge rate of 0.1 C with cut-off potentials at 0.1 V and 2 V versus Li/Li^+. As seen from Fig. 3a, the plateau at approximately 0.8 V in the first discharge curve for the MWCNTs electrode may be related to the formation of a passivation film or solid electrolyte interphase (SEI) on the carbon surface [20]. Li^+ insertion into MWCNTs took place mainly below 0.4 V. A first discharge capacity of 1082 mAh g^{-1} is much larger than the maximum theoretical specific charge of graphite, 372 mAh g^{-1}. The first charge capacity of 211 mAh g^{-1} responded to a large irreversibility efficiency of 80.5%, which was contributing to the formation of SEI [13].

As seen in Fig. 3b, sample SC1a shows a mixture of discharge/charge character of SnO_2 and MWCNTs, due to its small content of SnO_2. During the first reduction, the plateau present about 1.25 V and 0.95 V can be assigned to the formation of SEI layers on MWCNTs and the reduction of SnO_2, which lead to the formation of Sn(0) and of the insulating Li_2O [22,23]. The formation of Li_xSn alloys and lithium intercalation into graphite mainly occur below 0.75 V. The two processes can be described as the following reaction:

$$SnO_2 + 4Li + 4e^- \rightarrow 2Li_2O + Sn \quad (1)$$

$$Sn + xLi + xe^- \rightarrow Li_xSn \quad (2)$$

Reaction (1) is generally considered irreversible, thus the total reversible capacity is often defined as 781 mAh g^{-1} by considering only reactions (2). The plateau assigned to the formation of SEI layers on MWCNTs for SC2a electrode became smaller than that of SC1a electrode and even dismissed for SC3a and SC4a electrodes, because of the increasing content of SnO_2 in the composites. This result indicates that the coating of SnO_2 may hinder/reduce the SEI formation on the surface of MWCNTs for the SnO_2/MWCNTs electrodes; hence it can reduce greatly the irreversible capacity, and improve the charge capacity at the same time [20]. The discharge/charge curves for SC3a and SC4a electrodes are very similar. Due to the increasing amount of SnO_2, their potential plateaus scaled from 1.1 V to 0.9 V are much longer than that of SC1a and SC2a in the first discharge curve.

The initial discharge capacities are 1000 mAh g^{-1}, 1265 mAh g^{-1}, 1520 mAh g^{-1}, and 1460 mAh g^{-1} for SC1a, SC2a, SC3a and SC4a, respectively, which all exceed the theoretical capacity of SnO_2. The initial efficiencies of these electrodes are 45.4%, 49.6%, 47.5%, and 50.1%, respectively. The large irreversibility efficiency for the first cycle results from the following two reasons [24,25]: the first is that two Li^+-ions per oxygen

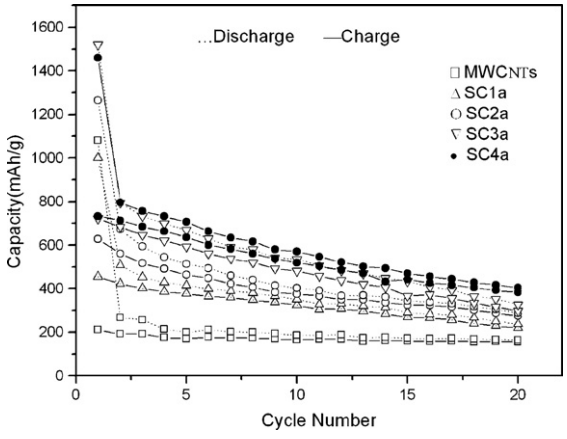

Fig. 4. Cycling performance of MWCNTs and SnO_2/MWCNTs in the 0.1–2 V (vs. Li^+/Li) voltage window at charge rate of 0.1 C.

atom are irreversibly trapped in the formation of Li_2O, which occupy almost 710 mAh g^{-1} as shown in reaction (1); the second is the formation of SEI film on the surface of MWCNTs and nascent Sn.

The electrochemical cycle properties of the SnO_2/MWCNTs composites over 20 cycles at the charge rate of 0.1 C are compared in Fig. 4. In terms of cyclability, the initial specific capacity decreased to 237 mAh g^{-1}, 288 mAh g^{-1}, 326 mAh g^{-1}, and 404 mAh g^{-1} after 20 cycles, corresponding to 23.7%, 22.8%, 21.4%, and 27.7% retention of the initial capacity for SC1a, SC2a, SC3a, and SC4a, respectively. As discussed above, if the large initial irreversibility capacity contributing to the reduction of SnO_2 is considered, the charge capacity decreased to 219 mAh g^{-1}, 275 mAh g^{-1}, 298 mAh g^{-1}, and 383 mAh g^{-1} after 20 cycles, corresponding to 48%, 44%, 41%, and 52% retention of the initial charge capacity for sample SC1a, SC2a, SC3a, and SC4a, respectively. It can be seen that the capacities increase with the increasing of SnO_2 amount in the composites, but the cycle efficiency can remain high for different samples. This could be ascribed to the good dispersion of SnO_2 on MWCNTs and the thin layer produced or small particle size, which is benefit to the utilization of SnO_2 and release of the stress caused by the drastic volume variation during the lithium intercalation/deintercalation process.

4. Conclusions

SnO_2/MWCNTs composites with smooth and uniform SnO_2 coating can be prepared by a novel thioglycolic acid assisted one-step wet chemical method. The thickness of SnO_2 coatings can be easily controlled by changing the synthesis conditions, such as pH value of the solution and hydrolysis time. The composites showed a good lithium intercalation/deintercalation performance when used as anode materials for lithium-ion batteries. Their high charge capacities and durability against decay are ascribed to the good dispersion of SnO_2 on MWCNTs and small particle size, which is benefit to the utilization of SnO_2 and release of the stress caused by the drastic volume variation during the lithium intercalation/deintercalation process.

Acknowledgements

This work was financially supported by the Beijing Natural Science Foundation (Grant No. 207001), the Beijing Science and Technology Program (Grant No. Z0004106040431), Funding Project for Academic Human Resources Development in Institutions of Higher Learning Under the Jurisdiction of Beijing Municipality, and the National 973 Program of China (Grant No. 2002CB211807). We thank Xu Xuedong and Xiao Weiqiang (Beijing University of Technology, Institute of Solid and Microstructure) for their kind help in TEM and XRD analysis.

References

[1] G. Faglia, C. Baratto, G. Sberveglieri, Appl. Phys. Lett. 86 (2005) 011923.
[2] B.V. Bergeron, A. Marton, G. Oskam, G.J. Meyer, J. Phys. Chem. B 109 (2005) 937–943.
[3] P.G. Harrison, C. Bailey, W. Azelee, J. Catal. 186 (1999) 147–159.
[4] U. Prüsse, M. Hähnlein, J. Daum, K.D. Vorlop, Catal. Today 55 (2000) 79–90.
[5] A. Yu, R. Frech, J. Power Sources 104 (2002) 97–100.
[6] J.N. Xie, V.K. Varadan, Mater. Chem. Phys. 91 (2005) 274–280.
[7] Y. Idota, T. Kubota, A. Matsufuji, Y. Maekawa, T. Miyasaka, Science 276 (1997) 1395–1397.
[8] H. Li, X.J. Huang, L.Q. Chen, Z.G. Wu, Y. Liang, Electrochem. Solid State Lett. 2 (1999) 547–549.
[9] J.Y. Lee, R.F. Zhang, Z.L. Liu, Electrochem. Solid State Lett. 3 (2000) 167–170.
[10] W.H. Lee, H.C. Son, J. Reucroft, J.G. Lee, J.W. Park, J. Mater. Sci. Lett. 20 (2001) 39–41 (0050).
[11] C. Kim, M. Noh, M. Choi, J. Cho, B. Park, Chem. Mater. 17 (2005) 3297–3301.
[12] Y. Wang, J.Y. Lee, Electrochem. Commun. 5 (2003) 292–296.
[13] Y. Wang, J.Y. Lee, J. Power Sources 144 (2005) 220–225.
[14] Y. Wang, J.Y. Lee, B.H. Chen, Electrochem. Solid State Lett. 6 (2003) A19–A22.
[15] N. Li, C.R. Martin, B. Scrosati, Electrochem. Solid State Lett. 3 (2000) 316–318.
[16] R. Retoux, T. Brousse, D.M. Schleich, J. Electrochem. Soc. 146 (1999) 2472–2476.
[17] S.C. Nam, Y.H. Kim, W.I. Cho, B.W. Cho, H.S. Chun, K.S. Yun, Electrochem. Solid State Lett. 2 (1999) 9–11.
[18] J. Read, D. Foster, J. Wolfenstine, W. Behl, J. Power Sources 96 (2001) 277–281.
[19] Y. Wang, F.B. Su, J.Y. Lee, et al., Chem. Mater. 18 (2006) 1347–1353.
[20] M.H. Chen, Z.C. Huang, G.T. Wu, G.M. Zhu, J.K. You, Z.G. Lin, Mater. Res. Bull. 38 (2003) 831–836.
[21] L.P. Zhao, L. Gao, Carbon 42 (2004) 1858–1861.
[22] T. Brousse, R. Retoux, U. Herterich, D.M. Schleich, J. Electrochem. Soc. 145 (1998) 1–4.
[23] R.A. Huggins, Solid State Ionics 113–115 (1998) 57–67.
[24] M. Wachtler, J.O. Besenhard, M. Winter, J. Power Sources 94 (2001) 189–191.
[25] I.A. Courtney, W.R. McKinnon, J.R. Dahn, J. Electrochem. Soc. 146 (1999) 59–68.